USE OF GLASS FIBER REINFORCED POLYMER EXTERNAL REINFORCEMENT IN CONSTRUCTION AND REPAIR OF REINFORCED CONCRETE LIQUID CONTAINMENT STRUCTURES

Manuel Paredes G.[a]*, Manuel F. Herrador[a], Ismael V. Raña[a], Iris González Taboada[a]

[a] *Escuela Técnica Superior de Ingenieros de Caminos Canales y Puertos, Universidade da Coruña*
**manuel.paredes@udc.es*

Keywords: Bond, reinforced concrete, GFRP, direct tension

Abstract
In this paper the behavior of reinforced concrete externally strengthened with GFRP under pure tensile loads is studied, from the point of view of its cracking performance and water tightness under service-level load values. A specific study,of bond behavior between strengthening and concrete is also provided. Tensile tests on reinforced concrete specimens externally strengthened with GFRP are performed in two phases:(1) specimens with or without external strengthening are tested up to cracking; (2) cracked specimens are strengthened and retested. The results obtained experimentally are compared to a numerical analysis. To analyze the bonding behavior between the strengthening and the concrete, tensile tests are carried out on a specifically designed specimen. For these tests modes of delamination, ultimate bond strength, mechanical behavior of the fiber and influence of the width and length are discussed.

1. Introduction

In this paper the use of external reinforcement of Glass Fiber Reinforced Polymer (GFRP) in construction, repair and strengthening of reinforced concrete axisymmetric liquid retaining structures is analyzed. The presence of horizontal tensile stresses in the concrete walls of the axisymmetric tanks cause an intensification of cracking. The structural design is based on the control of cracking up to acceptable values from the point of view of the durability and water tightness of the structure. Exposure to water and air, and the presence of aggressive chemical species can induce corrosion of the steel reinforcement or attack the concrete [1].

GFRP have characteristics that make them suitable for these structures. Exposure to saline environments, alkali, drying cycles, UV rays or influence of tropical temperatures, do not alter significantly their resistance [2-4], although freeze-thaw cycles might [5]. GFRP have high elongation capability, which makes them suitable as reinforcement from the point of view of cracked concrete waterproofing [6]. A small thickness external strengthened in reinforced concrete pieces reduces the strain of cracked components, reducing the width of the transverse cracks in the concrete [7].

Cracking and subsequent crack growth have a great importance in the behavior of concrete. The study of crack evolution after concrete failure cannot be performed with the use of simplified design models, which are often based on limitation of characteristic crack width of the steel stress. Concrete models based on the energy required for crack opening, which is a characteristic of the material, using concepts of brittle fracture [8-13], are efficient and applicable directly to the finite element model. This method does not only explains the growth of existing cracks, but also explains the development of new cracks at the moment when the tensile reaches cracking, and it is not necessary to make a dense mesh where the crack is created, reducing computation costs.

Since in this case GRPF is to be used as reinforcement in liquid retaining structures, a matrix compatible with the use for human consumption must be used. This reinforcement has low bonding to concrete. Therefore a specific bonding test campaign is performed. Diverse studies ([14], [15]) conclude that the adhesive strength model developed by Chen et al. (2001) [16] is valid and reliable. Since the type of bond between concrete and GFRP proposed in this paper does not coincide with any other in the database used for calibration of the model, the new results will be used to provide a new fitting for the general model.

2. Research plan

2.1. Description of tests and characterization of materials

The specimens present a shape similar to the section of a double T-beam, with parts in which the width is linearly reduced. The central area is smaller in order force crack formation in this area. To ensure cracking occurs in the center of the piece, where strain sensors are placed, two crack inducers are installed in that area. Dimensions are shown in Figure 1.

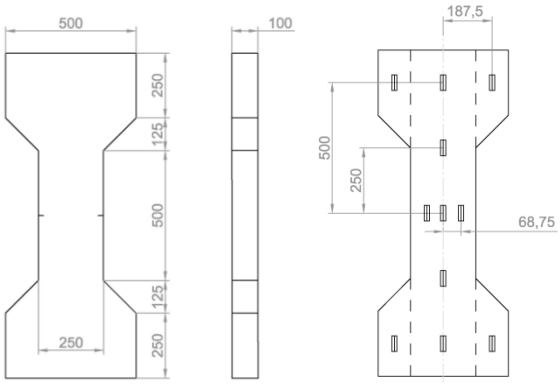

Figure 1: Specimen dimensions and location of the strain gages.

Tests have been conducted on 12 pieces with different reinforcements, external strengthenings and initial cracks in order to isolate different phenomena that interact in the global behavior of the element. Regarding the amount of reinforcement to be used, 3 situations are considered: using the minimum reinforcement under the Spanish EHE-08 code [17] with collapse criterion, in which the resistant steel section must be mechanically equivalent to the resistant concrete section under tensile stress (in this case 3.02 cm^2, 0.012 ratio), using approximately half of this minimum requirement (1.70 cm^2, 0.007 ratio), and plain concrete. For each one of the above cases a pair of pieces with external GFRP strengthening and another pair without it were tested. Once the latter were cracked under load, they were strengthened and tested in order to simulate the repair of damaged structures. Tests were performed under displacement

control at a constant speed of 0.2 mm/min to the actuator. Once the tests were performed, one core of each reinforced piece was extracted to perform a water penetration test under pressure, following the standard EN 12390-8:2009.

The external strengthening is a unidirectional fiberglass fabric with the same width as the central area of the piece and covers its entire length. The matrix used is Aquapox SR8500/SD2324, a bicomponent epoxy resin approved for alimentary use, with compressive strength of 42-49 MPa and elastic modulus of 2300 to 2400 MPa. Reinforcement is Gavazzi PV23-09, with 907 g/m^2 of glass fiber in the main direction, with a tensile strength of 3500 MPa and elastic modulus of 75000 MPa. The average thickness of the of the GFRP strengthening is 0.93 mm. Mechanical parameters of the materials are obtained by characterization tests. The average values of strength and elastic modulus of concrete are 61.75 MPa and 35400 MPa respectively, while in GFRP is 385 MPa and 16000 MPa respectively.

2.2. Description of finite element model

Commercial software Abaqus was used to develop the finite element model [18]. The finite element mesh is shown in Figure 2. The physical properties of concrete and GFRP are obtained from the results of laboratory tests (section 2.1). A post-failure behavior model of concrete based on the energy absorption by the material in the formation and subsequent growth of the crack [8-13] is used. The tensile strength of concrete was obtained in the characterization tests (4.48 MPa). Other model parameters were adjusted based on the results of tests on pieces with minimum reinforcement and external strengthening, using the other tests as a validation benchmark. The reason for this choice is that in the pieces without external strengthening, strain gages are placed directly on the concrete, and when the specimen cracks, the gages break. In the pieces with external strengthening, gages are placed on the fiber, preventing their breaking due to the elongation capability inherent to GFRP.

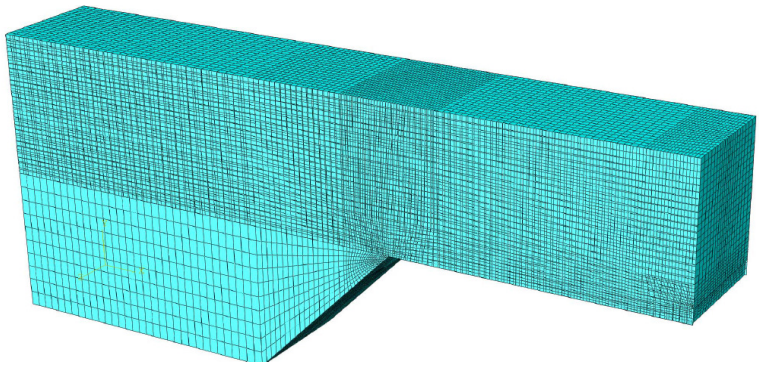

Figure 2. Finite element mesh.

3. Results

3.1. Tests results

3.1.1. Tests on pieces without cracking

In externally strengthened specimens, cracking load increases with the reinforcement ratio. The presence of external strengthening of GFRP also produces an increase in cracking load (Table 1).

	Minimum reinforcement	Reduced reinforcement	Without reinforcement
With strengthened	71.5 KN	67.0 KN	59.0 KN
Without strengthened	50.0 KN	50.0 KN	58.5 KN

Table 1. Cracking load for each speciment type

In specimens with or without external GFRP strengthening, the stress withstood by the concrete before cracking also increases with the reinforcement ratio (Table 2). Additionally, the presence of external strengthening increases the tension withstood by the concrete before cracking. Results for pieces with reinforcement ratio of 3.02 cm^2 are not shown because strains could not be recorded due to technical problems.

		Minimum reinforcement	Reduced reinforcement	Without reinforcement
With strengthened	Concrete	2.90 MPa	2.81 MPa	2.52 MPa
	Steel	16.37 MPa	15.86 MPa	-
	Fiber	1.31 MPa	1.27 MPa	1.14 MPa
Without strengthened	Concrete	-	2.64 MPa	1.79 MPa
	Steel	-	14.90 MPa	-

Table 2. Average stress value in each material at the cracking point.

3.1.2. Tests on strengthened pieces after cracking

In these pieces, the concrete specimen is cracked in the central zone, and the stress is resisted only by the longitudinal reinforcement and the external GFRP strengthening. On account of the greater tensile strength of these materials compared to concrete, load values higher than cracking of concrete value are reached, all without compromising the integrity of the piece. As the test advances, generation of new cracks along the piece is observed. Figure 3 shows a graph with the results.

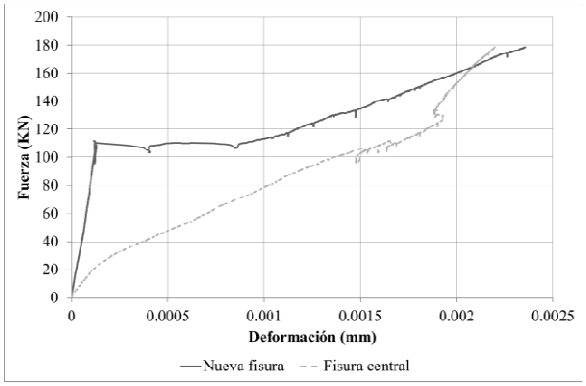

Figure 3. Central crack evolution and generation of new crack in cracked pieces and later strengthened

3.1.3. Permeability tests

The permeability test is performed on cores following standard test EN 12390-8:2009. These cores are 15 cm diameter and they are extracted from the central area of specimens loaded up to concrete cracking after placing of the external GFRP strengthening.. As benchmark, two cores without external strengthening pieces and uncracked zone are extracted. The depth of water penetration in these reference specimens is 25 mm. In tests on cores from reinforced

parts there is no water penetration was observed on externally reinforced cores except for one, which presented a small, 15 mm deep water incursion which was attributed to damage caused during the extraction of the core. Figure 4 shows the reference cores and the cores with GFRP.

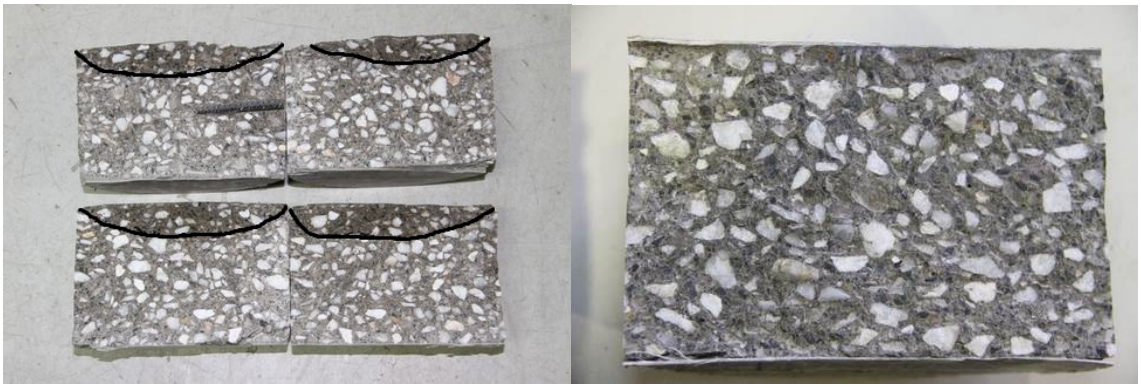

Figure 4. Left: water penetration into reference cores; right: cores from strengthened specimens, without water penetration.

3.2. Numerical analysis

In Table 3, the cracking load values obtained in the previously described numerical analysis are shown. The results obtained significantly match the values obtained in the tests. The most significant deviations occur in the pieces without external strengthening and with reinforcement, in which the experimental results are lower than in the pieces without reinforcement. These results do not coincide with theoretical concepts of reinforced concrete, so a new series of tests has been proposed and is to be carried out to confirm these results.

		Minimum reinforcement	**Reduced reinforcement**	**Without reinforcement**
With strengthening	Test value	71.0 KN	67.0 KN	59.0 KN
	Numerical value	71.4 KN	67.2 KN	62.5 KN
	Deviation	0.14%	0.30%	5.60%
Without strengthening	Test value	50.0 KN	50.0 KN	58.5 KN
	Numerical value	63.6 KN	63.0 KN	59.0 KN
	Deviation	27.10%	26.00%	0.85%

Table 3. Comparison between experimental values and numerical results.

The maximum stress values of longitudinal reinforcement and external strengthening are 31.40 MPa and 11.60 MPa respectively. They are much lower than the yield strength of each of them, 500 MPa in steel and 385 MPa in GFRP.

4. Bonding tests

4.1. Bonding tests description

The test device is formed by two concrete cylinders, of 15 cm diameter and 25 cm high. Each one a steel bar embedded to transmit tensile forces to the concrete by bonding between both materials (Figure 5). The cylinders were joined by three GFRP bands at 120º.

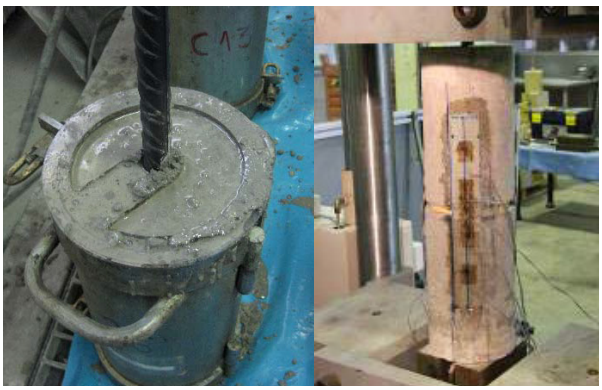

Figure 5. Concrete specimen with embedded steel bar (left) and fully mounted device (right).

Tests with different widths and lengths of fiber, plus a set with external transverse strengthening at the end, were carried out. Table 4 shows the different parameters. Five gages on each reinforcement are placed, one in the central part of the band and symmetrically on both sides, one at L/4 distance and another at 5L/8 distance of the central plane.

	Nº specimens	**Fiber width (b, mm)**	**Transverse reinf.**	**Bond length (L, mm)**	**L/b**	**Total length (mm)**
Type I	4	45	NO	135	3	280
Type II	4	45	NO	150	3.33	310
Type III	4	55	NO	150	2.73	310
Type IV	4	55	NO	165	3	340
Type V	4	45	YES	135	3	280

Table 4. Description of the full set of bond tests.

4.2. Bonding tests results

The failure type which took place in all tests was the delamination at the adhesive-concrete interface. The process begins with a small concrete fracture in the center of the device and in the upper or lower cylinder. Fracture direction forms 45° (Figure 6) with the longitudinal axis of the strengthened. As the load increases, this fracture starts the delamination process, which is spread to the ends of the strengthening, and sometimes ends up by delaminating all the fiber. Fracture takes place on around 20-50% of the bonded length (Chen et al 2001 [4], Yao et al 2005 [8]).

Figure 6. Adhering concrete volume.

Analyzing the ultimate strength experimental values and the theoretical values provided by the formulation of the reference model [4], it can be concluded that the general model overestimates strength for this type of low-bond material. After the adjustment, the coefficient α obtained is α=0.318 instead of the original value 0.427. It was also observed that longer bonds over effective bond length did not contribute to ultimate strength, but contributed to improve the ductility of the failure mode.

5. Conclusions

The external GFRP strengthening increases the maximum tensile stress that concrete resists before cracking. Once a crack appears, it grows more slowly, allowing time to take appropriate actions if necessary. It also favors the water tightness of concrete structures. It can be used to repair a cracked concrete water tank, and it provides continuity along the crack making a section with higher tensile capacity.

The finite element model shows that cracking loads and behavior on the pieces agree with the values obtained in experimental tests. Therefore test format is deemed to be valid and the finite elements model is going to be used to future changes or evolution of next experimental tests.

An increase in the bonded length of the fiber provides greater ductility to the delamination process and an increase in width provides greater final strength to the ensemble. The fact that the reinforcement used has a lower than usual resistance and adhesion, makes the adjustment of the adhesive strength reference model [4] suitable for this type of failure.

Therefore, it can be concluded that the application of an external strengthening GFRP improves the behavior of reinforced concrete against pure tensile stresses, being recommended its application to the construction of water tanks.

A new set of tests with longitudinal reinforcement and without external GFRP strengthening, as well as a second series of benchmark tests is being carried out at prsent. New penetration tests on cracked test cores with ulterior external GFRP strengthening are also pending.

6. Acknowledgements

This project has been funded by the Programa Sectorial de Investigación Aplicada e I+D Suma 10TMT118004PR, “Análise da fisuración por tracción en depósitos de formigón armado revestidos con polímeros reforzados con fibra de vidro (AFIDHAVIT)”, Consellería de Educación e Ordenación Universitaria de la Xunta de Galicia, and project BIA2010 “Adherencia y anclaje de las armaduras pasivas en el hormigón. Hacia un modelo y una formulación general”, Proyectos de Investigación Fundamental del Ministerio de Ciencia e Innovación del Gobierno de España.

7. References

[1] Calavera J. *Patología de estructuras de hormigón armado y pretensado*. INTEMAC, Madrid, 2005.

[2] Almusallam T.H. Load-deflection behavior of RC beams strengthened with GFRP sheets subjected to different environmental conditions. *Cement and Concrete Composites*, vol 28, pp. 879-889, 2006.

[3] Almusallam T.H. Durability of GFRP rebars in concrete beams under sustained loads at severe environments. *Journal of Composite Materials*, vol 40, pp. 623-637, 2006.
[4] Hulatt J. Preliminary investigations on the environmental effects on newheavyweight fabrics for use in civil engineering. *Composites Part B: Engineering*, vol 33, pp. 407-414, 2002.
[5] Saenz N. Long term durability of strengthened concrete with externally applied FRP composites. *International SAMPE Symposium and Exhibition (Proceedings)*, vol 49, pp. 2953-2966, 2004.
[6] Delucchi M. Crack-bridging ability and liquid water permeability of protective coatings for concrete, *Progress in Organic Coatings*, vol 33, pp. 76-82, 1998.
[7] Ferretti D., Savoia M., Tension-stiffening law for FRP- reinforced concrete elements under service loadings, *Proc., Int. Symp., Bond Behaviour of FRP in Structures*, pp. 221–227, 2005.
[8] Hillerborg A., Modéer M., Petersson P.E. Analysis of crack formation and crack growth in concrete by means of fracture mechanics and finite elements, *Cement and Concrete Research*, vol 6, pp 773-781, 1976.
[9] Y. Xu, H. Yuan, Computational analysis of mixed-mode fatigue crack growth in quasi-brittle materials using extended finite element methods, *Engineering Fracture Mechanics*, vol. 76, no. 2, pp. 165–181, 2009.
[10] Zhang X.-F., Xu S:-L. Study on mechanical behavior of fracture process zone in concrete using energy approach, *Gongcheng Lixue/Engineering Mechanics*, Vol 25, pp 18-23, 2008.
[11] Wardeh G., Ghorbel E. Freezing-thawing cycles effect on the fracture properties of flow able concrete. *Proceedings of the 8th International Conference on Fracture Mechanics of Concrete and Concrete Structures*, pp 1818-1827, 2013.
[12] Héctor Cifuentes, Fidel García, Orlando Maeso, Fernando Medina, Influence of the properties of polypropylene fibres on the fracture behaviour of low-, normal and high-strength FRC, *Construction and Building Materials*, vol 45, pp 130-137, 2013.
[13] Hu S.-W., Mi Z-X, Lu J, Fan X.-Q, A study on energy dissipation of fracture process zone in concrete, *Journal of Hydraulic Engineering*, vol 43, pp 145-152, 2012.
[14] Teng JG, Smith ST, Yao J, Chen JF. Intermediate crack-induced debonding in RC beams and slabs, *Construction and Building Materials*, No. 17, pp. 447-462, 2003.
[15] Yao J, Teng JG, Chen JF. Experimental study on FRP-to-concrete bonded joints, *Composites: Part B 36*, pp. 99-113, 2005.
[16] Chen JF, Teng JG. Anchorage strength models for FRP and steel plates bonded to concrete, *ASCE Journal of Structural Engineering*, Vol 127, No. 7, pp. 784-91, 2001.
[17] Ministerio de Fomento, Instrucción de Hormigón Estructural. EHE-08, Centro de Publicaciones, Ministerio de Fomento, Madrid, 2008.
[18] Abaqus. Abaqus 6.12 user's manual. Abaqus, Inc., Providence, 2012.